

Research on a Lightweight and Intelligent Operation and Maintenance System for Small and Medium-sized Ships Driven by Digital Twins

Genyuan Wang¹, Xiaona Liu², Tairong Tian¹, Long Chen¹, Haidun Wang¹, Keqin Tang¹, Wenbo Li¹

¹School of Maritime, Hainan Vocational University of Science and Technology, Haikou 571126, Hainan, China

²Student Affairs Department, Hainan Vocational University of Science and Technology, Haikou 571126, Hainan, China

Copyright: © 2026 Author(s). This is an open-access article distributed under the terms of the Creative Commons Attribution License (CC BY 4.0), permitting distribution and reproduction in any medium, provided the original work is cited.

Abstract: To address the challenges of high deployment costs and limited edge computing power in intelligent retrofitting of small and medium-sized vessels, this study proposes a lightweight intelligent operation and maintenance (O&M) system architecture based on the digital twin five-dimensional model framework. The architecture features a five-layer collaborative architecture comprising “physical entity—virtual entity—service system—twin data—connection.” At the physical entity layer, a low-cost multi-source data acquisition platform is implemented using an Arduino Uno R3 integrated with a DS18B20 temperature sensor and SW-420 vibration sensor. The virtual entity layer employs the Three.js engine to achieve real-time 3D scene rendering and virtual-real mapping, reducing model loading time from 3.2 seconds to 1.8 seconds while maintaining an average rendering frame rate of 24 FPS. The service system layer integrates functions for status monitoring, threshold alerts, and fault classification inference. The twin data layer combines 500 samples from public datasets and laboratory-collected data to construct a four-dimensional feature space. The connection layer enables end-to-end data synchronization via USB serial port and WebSocket protocol. For fault diagnosis, a random forest classifier performs ternary classification of equipment status (normal/overtemperature/anomalies), achieving an overall accuracy of 71% and a normal state recall rate of 78% after hyperparameter optimization. Analysis of the physical mechanism underlying the confusion matrix reveals that the cross-false judgment between vibration anomalies and excessive temperature stems from the frictional heat generation coupling effect induced by bearing wear, highlighting the limitations of feature separability when relying on a single sensor dimension in multi-fault-mode coupling scenarios. From the perspective of the Nyquist sampling theorem, this study demonstrates the fundamental constraints of the current 1 Hz sampling rate on vibration feature capture. The prototype system’s hardware cost is kept below ¥200, with power consumption under 5W, verifying the technical feasibility of implementing core digital twin functionalities under constrained edge computing resources.

Keywords: Digital twin; Five-dimensional model; Intelligent ship operation and maintenance; Edge computing; Random forest; Fault diagnosis; Lightweight architecture

Online publication: March 26, 2026

1. Introduction

The global shipping industry is undergoing a paradigm shift from “experience-driven” to “data-driven.” The International

Maritime Organization (IMO) 's 2023 revised Technical Guidelines for the Energy Efficiency Index (EEXI) and the Carbon Intensity Index (CII) rating system impose mandatory compliance requirements for energy efficiency management of existing vessels^[1,2]. According to statistics from the Maritime Safety Administration of China's Ministry of Transport, small and medium-sized bulk carriers, general cargo ships, and oil and chemical carriers with a tonnage of 3,000 to 10,000 tons account for over 70% of China's registered vessels. However, their adoption rate of intelligent technologies remains below 10%, with widespread issues such as delayed fault response, crude energy consumption management, and heavy reliance on individual experience of engineers for operational decisions. Small and medium-sized vessels face three major technical challenges in adopting intelligent solutions: first, the economic disparity between the deployment cost of industrial-grade digital twin platforms (typically exceeding one million US dollars) and the limited capital of small and medium-sized shipping enterprises; second, the technical challenge between high-precision sensor arrays and the limited computing power and low-bandwidth communication capabilities at the edge; and third, the management conflict between increasingly stringent IMO compliance requirements and the current rudimentary operational practices. These challenges constitute the core technical barriers to the intelligent transformation of small and medium-sized vessels.

Digital Twin technology provides a new theoretical framework for intelligent ship operation and maintenance. The five-dimensional Digital Twin model proposed in existing research, comprising physical entity (PE), virtual entity (VE), service system (SS), twin data (DD), and connectivity (CN), has been widely applied in aerospace and smart manufacturing sectors, while research in ship engineering remains in its exploratory stage^[3]. Relevant studies systematically review the current applications of Digital Twin technology in ship maintenance, noting that current research primarily focuses on structural health monitoring and energy efficiency optimization for large commercial vessels, with lightweight solutions for small and medium-sized ships still lacking^[4]. Another study proposed a deep convolutional neural network-based fault prediction method for ship engines, achieving high classification accuracy on public datasets; however, the approach relies on high-performance GPU servers and large-scale annotated datasets, making it difficult to deploy in edge computing environments for small and medium-sized ships^[5]. Some studies validated the effectiveness of random forest algorithms in rotating machinery fault diagnosis but failed to conduct adaptive analyses tailored to the unique operating conditions of ship engines (e.g., wide-speed fluctuations, broadband cabin vibration noise superposition, and salt spray corrosion environments)^[6]. Related research developed NB-IoT-based remote ship monitoring systems with reference value at the communication protocol level, but did not address intelligent device status analysis^[7]. Some studies have proposed digital twin-based methods for predicting the remaining service life of marine diesel engines; however, these approaches rely heavily on extensive historical degradation data and are unsuitable for small and medium-sized vessels with limited data availability^[8]. Overall, existing research faces three major challenges: high cost barriers, heavy data dependency, and poor industry adaptability. Notably, there is a significant lack of engineering practices that enable effective condition monitoring through low-cost sensing in environments with limited edge computing resources and low-bandwidth communications.

Based on the aforementioned analysis, this paper adopts the core concept of "lightweight digital twin" to develop an intelligent operation and maintenance prototype system for small and medium-sized vessels under undergraduate laboratory conditions. Key innovations include: establishing a five-layer collaborative architecture ("PE-VE-SS-DD-CN") based on the five-dimensional digital twin model, which integrates previously discrete hardware acquisition, 3D visualization, and fault diagnosis modules into a cohesive system, forming a complete closed-loop process from perception to mapping and decision-making; revealing, through in-depth analysis of the confusion matrix's physical mechanisms, the cross-misjudgment mechanism caused by the coupled effect of vibration anomalies and excessive temperature due to heat generation from bearing wear friction, as well as the Nyquist sampling limitation on vibration feature capture at a 1 Hz sampling rate; and demonstrating the technical feasibility of implementing basic digital twin functionalities with hardware costs under 200 yuan despite limited edge computing resources, providing a replicable technical pathway for cost-effective intelligent retrofitting of small and medium-sized vessels.

2. System architecture design

2.1. Overall architecture based on the five-dimensional model

Building upon the five-dimensional digital twin model proposed in existing research, this system establishes a five-layer collaborative architecture comprising “physical entity—virtual entity—service system—digital twin data—connection”^[3]. The core concept of the five-dimensional model lies in the fact that its components are not merely hierarchically stacked but form a closed-loop driven by data flows: the operational status of the physical entity is transmitted in real-time to the digital twin data layer via the connection layer; the digital twin data is analyzed and inferred by the service layer to generate decision-making insights; these insights are then relayed downward through the connection layer to the virtual entity layer for visualization, while simultaneously feeding back to the physical entity layer to guide operational maintenance activities. Compared to the traditional three-layer “collection–processing–application” architecture, the five-dimensional model emphasizes real-time virtual-physical mapping and the integrity of the decision-making closed-loop, thereby more accurately capturing the essential characteristics of digital twin systems.

The primary data flow path is as follows: The physical entity layer generates raw temperature and vibration data at a 1 Hz sampling rate, which is transmitted to the host computer via a USB serial port. The host computer’s data preprocessing module removes outliers and applies sliding-window smoothing. It then stores the raw data in the historical database of the twin data layer while extracting a four-dimensional feature vector for input to the fault classification inference engine in the service layer. The classification results and confidence scores generated by the inference engine are sent via the WebSocket protocol to the front-end interface of the virtual entity layer, triggering updates to the status indicators for the corresponding equipment areas in the 3D scene (normal status shown in green, alarm status in red). Measured end-to-end latency in laboratory conditions is approximately 120 ms, meeting the time-scale requirements for near-real-time monitoring.

2.2. Physical entity layer

The core of the physical entity layer is a scaled-down simulation platform designed to replicate typical operating conditions and fault modes of marine main engines. Centered around a 12V/3,000 rpm DC motor as the primary drive component, the platform utilizes a PWM speed control module to achieve continuous speed regulation across the 800–3,000 rpm range, accurately simulating rotational speed fluctuations under various operational scenarios, including port entry/exit, variable-speed navigation, and sudden load variations. Temperature sensors (DS18B20 × 2) are applied via thermal grease between the motor housing’s drive and non-drive surfaces to measure radial temperature distribution, while vibration sensors (SW-420) are mounted near the bearing housing using mechanical clamps to capture radial vibration signals. The sensor data is converted by an Arduino Uno R3 ADC and transmitted to the host computer via a USB serial port at a sampling rate of 1 Hz.

It is particularly noteworthy that several interference factors present in the actual operating environment of marine main engines cannot be simulated under laboratory conditions: (1) The engine room background temperature can reach 45–55°C, significantly higher than the laboratory reference temperature of 25°C, which may cause zero drift and sensitivity variations in temperature sensors; (2) The hull structural vibrations induced by engine operation exhibit broadband random vibrations (frequency range: 10–2,000 Hz), whereas laboratory vibrations primarily originate from the periodic rotation of the motor itself; these two types of vibrations differ fundamentally in their spectral characteristics; (3) The corrosive effects of marine salt spray on electronic components substantially reduce sensor lifespan and measurement accuracy. These factors constitute the primary sources of uncertainty when extrapolating experimental results to real-world ship operating conditions.

2.3. Virtual entity layer

The virtual entity layer handles the rendering of virtual-to-real-world mapping and human-computer interaction. The 3D hull model, modeled parametrically using Blender software with a small bulk carrier as the reference, was optimized

topologically and exported in glTF format, reducing the file size from 2.1 MB to 0.8 MB. The front-end interface, built with the Three.js engine, enables six-degree-of-freedom interaction with the hull model and integrates the Chart.js component to plot temperature time-series curves. When sensor data exceeds preset alert thresholds, the corresponding equipment area in the scene is highlighted in red with an alert message displayed, achieving a “what-you-see-is-what-you-get” synchronization between virtual and real-world representations.

2.4. Service system layer

The service system layer encapsulates three core functional modules: (1) Status Monitoring Service: Responsible for real-time reception, circular buffer caching, and forwarding of sensor data; (2) Threshold Alert Service: Instantly identifies abnormal states based on predefined rules and sends alert messages; (3) Fault Classification Inference Service: Calls the random forest model to generate ternary classification results and prediction probabilities. These service modules achieve loosely coupled integration through RESTful APIs and WebSocket interfaces.

2.5. Student data layer and connection layer

The twin data layer integrates a public dataset (300 samples) with laboratory-collected data (200 samples), totaling 500 samples. Each sample contains four feature dimensions: mean temperature μ_T , temperature standard deviation σ_T , vibration amplitude V_{amp} , and rotational speed n , labeled under three operational states: normal (C_0), excessively high temperature (C_1), and abnormal vibration (C_2). The connection layer transmits data via a USB serial port at a sampling rate of 1 Hz and has successfully completed feasibility testing for remote transmission using the MQTT protocol.

3. Fault diagnosis model

3.1. Feature engineering

Feature engineering serves as the foundational work for the performance of fault diagnosis models. This study extracts four-dimensional feature vectors from a time-domain statistical perspective, with the physical meanings of each feature as follows.

- (1) Average temperature μ_T . It reflects the thermal equilibrium state of the equipment during the sampling period. When the cooling system efficiency declines or the friction pair experiences abnormal wear, μ_T shows a continuous upward trend. For marine main engines, key monitoring parameters include the cylinder liner cooling water temperature and supercharger exhaust temperature.
- (2) Temperature standard deviation σ_T . It characterizes the degree of temperature fluctuation within the sampling window. Under normal operating conditions, the equipment temperature fluctuates slightly around the steady-state value, resulting in a small σ_T ; however, when cooling conditions change abruptly or intermittent friction occurs, σ_T increases significantly.
- (3) V_{amp} (vibration amplitude). For the SW-420 digital sensor, V_{amp} is defined as the ratio of the high-level duration within the sampling window to the total sampling duration, i.e., the vibration trigger rate. Mechanical faults such as bearing wear or rotor imbalance will cause a significant increase in V_{amp} .
- (4) Rotation speed n . Used as a proxy variable for operating load. The rotation speed of the ship’s main engine varies significantly under different navigation conditions, and its variations directly affect vibration characteristics and thermal load; therefore, it is incorporated into the feature space to control operational mixing factors.

Feature extraction employs a sliding window mechanism: the window length is set to 30 seconds with a step size of 1 second, during which statistical feature values are calculated within the window.

3.2. Random forest classifier

This study compares three classification algorithms: Decision Tree, Random Forest, and Support Vector Machine (SVM).

Random Forest makes classification decisions through a Bagging voting mechanism that integrates multiple decision trees, demonstrating good generalization ability and overfitting resistance in small sample scenarios. The model is implemented using the Python scikit-learn library, with a stratified split of the dataset into training and test sets at an 80/20 ratio. Key hyperparameters: $n_estimators = 100$, $max_depth = 5$.

4. Experiments and result analysis

4.1. Experimental dataset

The experimental dataset is composed of a fusion of publicly available data (UCI Machine Learning Database, 300 samples) and laboratory-collected data (200 samples), totaling 500 samples. Among these, 280 samples (56%) represent normal conditions, 120 samples (24%) indicate excessive temperature, and 100 samples (20%) show abnormal vibration. The statistical characteristics of the dataset are presented in **Table 1**.

Table 1. Statistical characteristics of the dataset

Feature	Mean	Standard deviation	Least value	Crest value
Temperature /°C	48.6	15.3	25.1	89.7
Standard deviation of temperature /°C	3.2	2.1	0.4	8.6
Vibration amplitude	0.35	0.28	0.05	0.92
Rotational speed / (r·min ⁻¹)	1 850	620	800	3 000

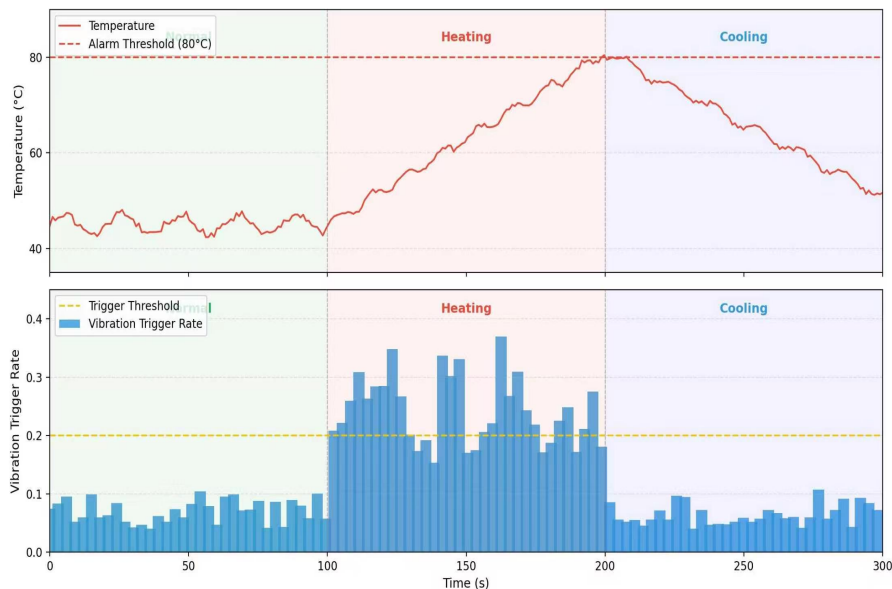


Figure 1. Sensor data time series (simulated experimental data).

Figure 1 illustrates the typical temporal variations of temperature and vibration signals during the simulation experiment. During the normal operation phase from 0 to 100 seconds, the temperature stabilized around 45°C with a vibration trigger rate close to zero; from 100 to 200 seconds during the heat source loading stage, the temperature continuously rose above 80°C, and the vibration trigger rate increased due to changes in bearing clearance caused by motor thermal expansion; the period from 200 to 300 seconds corresponded to the cooling recovery phase. This temporal curve visually demonstrates the characteristic differences between normal and abnormal operating conditions.

4.2. Classification performance analysis

The Random Forest classifier achieved an overall classification accuracy of 71% on the test set, with weighted average precision, recall, and F1 score all at 0.71. **Table 2** presents detailed classification performance metrics for each category, while **Table 3** shows the corresponding confusion matrices.

Table 2. Performance report of the random forest classifier

Class	Precision	Recall	F1 value	Support Count
Normal (C ₀)	0.76	0.78	0.77	48
Hyperpyrexia (C ₁)	0.72	0.70	0.71	30
Vibration anomaly (C ₂)	0.63	0.62	0.63	22
weighted mean	0.71	0.71	0.71	100

Table 3. Confusion matrix

Actual Category \ Predicted Category	Predict C ₀	Predict C ₁	C ₂ Prediction
Actual C ₀ (normal)	39	5	4
Actual C ₁ (temperature is too high)	4	21	5
Actual C ₂ (vibration anomaly)	3	6	13

The confusion matrix reveals two distinct types of misjudgment patterns with physical significance.

- (1) Cross-failure classification between abnormal vibration (C₂) and excessive temperature (C₁): Six C₂ samples were misclassified as C₁, while five C₁ samples were misclassified as C₂. From a physical failure mechanism perspective, mechanical faults such as bearing wear or rotor imbalance not only directly increase vibration amplitude but also cause localized temperature rise due to heat generation from friction between friction pairs, resulting in a “vibration-temperature” coupled response. Let the bearing friction torque be M_f and the rotational speed be n; the frictional heat power P_f can be approximated as:

$$P_f = 2\pi \cdot M_f \cdot n / 60$$

When bearing wear increases the friction torque M_f, the frictional heat generation power P_f rises correspondingly, manifested as a simultaneous increase in both the mean temperature μ_T and its standard deviation σ_T. In the current four-dimensional feature space that relies solely on time-domain statistical characteristics, the eigenvectors of these coupled failure modes exhibit significant overlap, making it difficult for the random forest to achieve effective separation at the decision boundary.

- (2) Misclassification from normal state (C₀) to abnormal vibration (C₂) (5 cases). The SW-420 vibration sensor employs binary output, and its threshold determination mechanism lacks continuous quantization capability, resulting in false triggering of normal vibration signals at the threshold boundary.

4.3. Theoretical analysis of sampling frequency restrictions

The current 1 Hz sampling rate imposes fundamental limitations in capturing the vibration characteristics of marine main engines. The dominant frequencies of vibration signals from these engines typically range between 10 and 500 Hz. According to the Nyquist sampling theorem:

$$f_s \geq 2 \cdot f_{\max}$$

For ship main engine vibration signals ($f_{\max} \approx 500$ Hz), the theoretical sampling frequency should be no less than 1 kHz. The current 1 Hz sampling rate is merely 1/1,000 of the theoretical minimum requirement, completely losing the frequency, phase, and waveform information of the vibration signals. Future upgrades to MEMS accelerometers (e.g., the MPU6050, with a sampling rate of up to 1 kHz), combined with FFT-based frequency-domain feature extraction, are

expected to significantly improve feature separability and classification accuracy.

4.4. Feature importance and model interpretability

Table 4. Feature importance ranking

Feature	Importance Score	Proportion /%
Average temperature μ_T	0.38	38
Vibration amplitude V_{amp}	0.31	31
Standard Deviation of Temperature σ_T	0.19	19
speed n	0.12	12

The mean temperature μ_T ranked first with a 38% significance score, followed by vibration amplitude V_{amp} at second place with 31%. When the significance scores of these two feature types are close and physically coupled, the classifier's decision boundary in their overlapping region becomes blurred, which is the root cause of cross-false judgments.

4.5. Visualization system performance

Table 5. Visualization system performance before and after optimization

performance index	Before Optimization	postoptimality
Model file size / MB	2.1	0.8
Model loading time/s	3.2	1.8
Average rendering frame rate/FPS	18	24

After optimization, the scene rendering frame rate has been increased to 24 FPS, ensuring smooth performance during rotation and scaling interactions. The aforementioned tests were conducted in a single-client, local network environment; however, network constraints in real-world ship environments may affect real-time performance.

4.6. System cost and power consumption

Table 6. Summary of hardware costs

Project	Cost/ Yuan	Remarks
Arduino acquisition module	170	Including sensors, motors, and auxiliary materials
Raspberry Pi (optional)	300	This project did not involve procurement; laptops were used instead.
Notebook PC	—	The team owns its own equipment, which is not included.
Total actual investment	170	Excluding labor costs

The entire collection-end hardware costs approximately 170 yuan, consumes less than 5W of power, and can be powered via a USB interface. Compared to industrial-grade ship condition monitoring systems, this solution offers a three-order-of-magnitude cost advantage.

5. Discussion

5.1. Comparative Analysis with Existing Solutions

Table 7. Comparison between the proposed method and representative methods

Scheme	Sensor Type	Sort algorithm	Precision	Hardware cost	Deployment Environment
This document proposal	DS18B20 + SW-420	random forest	71%	170 yuan	laboratory
Zhang Mingyuan et al. ^[5]	Industrial-grade array	degree of depth CNN	> 90%	> 100,000 yuan	Actual ship
Liu Chao et al. ^[8]	Multi-parameter sensor	LSTM	> 85%	Not Public	laboratory
Chen Qiang et al. ^[6]	acceleration transducer	random forest	89%	≈ 5 k yuan	Experiment Table

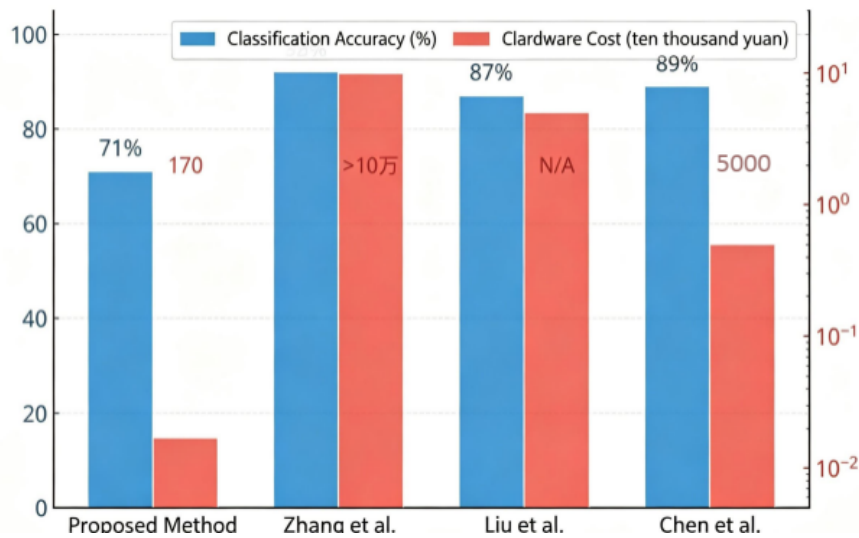


Figure 2. Performance-cost comparison between the proposed method and representative methods.

As shown in **Figure 2**, this solution exhibits a significant gap in classification accuracy compared to other approaches, yet offers a notable advantage in hardware cost (¥170 versus several thousand to hundreds of thousands of yuan). This combination of “low accuracy—low cost” represents an inevitable trade-off inherent in lightweight design. For small and medium-sized vessels, constrained by limited labeled data and limited high-performance computing resources, lightweight machine learning methods such as random forests provide a practical compromise solution that is “good enough”, its value lies not in achieving optimal accuracy, but in enabling basic state awareness at minimal cost, thereby facilitating data accumulation and decision-making support for subsequent phased upgrades.

5.2. Application prospects for IMO compliance

The EEXI technical guidelines, revised by the IMO in 2023 and the CII rating system impose clear energy efficiency compliance requirements on existing vessels. The low-cost condition monitoring technology approach validated by this prototype system can serve as an auxiliary tool for vessel energy efficiency monitoring in the future. The “Guidelines for Intelligent Vessel Navigation Inspection” issued by China Classification Society in 2024 specify the inspection framework for intelligent vessel operation and maintenance systems ^[9].

5.3. Limitations and improvement directions

The primary limitations of this prototype system include:

- (1) Sensor dimensionality constraints – the SW-420 only outputs binary signals and cannot quantify vibration amplitude and frequency;
- (2) Insufficient data representativeness – the sample size of 500 records is too small, with some data sourced from public datasets;
- (3) Lack of environmental adaptability – it does not simulate actual cabin conditions such as high temperature, high humidity, and salt spray corrosion;
- (4) Limited model generalization capability – the model has not undergone validation under real-ship operating conditions.

Future improvement directions:

- (1) Adopt MEMS sensors and increase the sampling frequency to the kHz range;
- (2) Explore transfer learning and domain-adaptive methods;
- (3) Implement IP65 or higher-level waterproof and dustproof hardware protection;
- (4) Collaborate with shipping companies to conduct ship-based pilot validation.

6. Conclusion

To address the challenges of high deployment costs and limited edge computing power in the intelligent transformation of small and medium-sized vessels, this paper proposes and implements a lightweight intelligent operation and maintenance (O&M) prototype system based on the five-dimensional digital twin model framework. The key findings are as follows.

- (1) A five-layer collaborative architecture has been established, encompassing “physical entities—virtual entities—service systems—twin data—connections,” forming a complete closed-loop process from perception to mapping to decision-making.
- (2) The overall classification accuracy of the random forest classifier was 71%, with a recall rate of 78% under normal conditions. Confusion matrix analysis revealed the misclassification mechanism between vibration anomalies and overheating-induced frictional heat generation.
- (3) The system hardware cost is kept below 200 yuan, with power consumption under 5W. The 3D visualization subsystem achieves an average rendering frame rate of 24 FPS and a loading time of 1.8 seconds.
- (4) Subsequent work will focus on sensor upgrades, feature space expansion, exploration of transfer learning methods, and validation through real-ship pilot tests.

Funding

2025 Hainan Provincial University Student Innovation Training Project, “Construction of an Intelligent Ship System Powered by Digital Twin Technology”

Disclosure statement

The authors declare no conflict of interest.

References

- [1] International Maritime Organization, 2023, 2023 Guidelines on the Method of Calculation of the Attained Energy Efficiency Existing Ship Index (EEXI). IMO, London.
- [2] International Maritime Organization, 2023, Initial IMO Strategy on Reduction of GHG Emissions from Ships. IMO,

London.

- [3] Tao F, Liu WR, Zhang M, et al., 2019, Five-Dimensional Digital Twin Model and Its Applications in Ten Major Fields. *Computer Integrated Manufacturing Systems*, 25(1): 1–18.
- [4] Wang JP, Chen ZG, Zhou Y, 2023, Review of the Application of Digital Twin Technology in Ship Operation and Maintenance. *Naval Architecture and Ocean Engineering*, 52(5): 45–53.
- [5] Zhang MY, Li HB, Wang ZC, 2024, A Method for Ship Engine Fault Prediction Based on Deep Convolutional Neural Networks. *China Navigation*, 47(2): 112–119.
- [6] Chen Q, Wang MH, Zhang JJ, 2023, Application Research of the Random Forest Algorithm in Mechanical Fault Diagnosis. *Vibration and Shock*, 42(6): 178–185.
- [7] Zhao W, Sun JG, Zhou P, 2024, Design of a NB-IoT-Based Ship Remote Monitoring System. *Journal of Sensor Technology*, 37(1): 89–96.
- [8] Liu C, Li YM, Wen GL, 2024, Digital Twin-Driven Remaining Useful Life Prediction for Marine Diesel Engine. *Ocean Engineering*, 291: 116468.
- [9] China Classification Society, 2024, Guidelines for Intelligent Navigation Inspection of Ships. China Classification Society, Beijing.
- [10] Lin HP, Zhang ZQ, 2024, Path Selection and Policy Recommendations for Intelligent Transformation of Small and Medium-Sized Ships. *Journal of Transportation Engineering*, 24(2): 156–165.
- [11] Zhang WM, Wang Y, Chen J, 2024, A Lightweight Edge Computing Framework for Ship Machinery Health Monitoring. *Journal of Marine Science and Engineering*, 12(3): 412.
- [12] Breiman L, 2001, Random Forests. *Machine Learning*, 45(1): 5–32.

Publisher's note

Whoice Publishing remains neutral with regard to jurisdictional claims in published maps and institutional affiliations.